Continental Shelf Research 31 (2011) 9–14

Contents lists available at ScienceDirect

Continental Shelf Research

journal homepage: www.elsevier.com/locate/csr

Currents in a small channel on a sandy tidal flat

Steve Elgar*, Britt Raubenheimer

Woods Hole Oceanographic Institution, Woods Hole, MA 02543, USA

ARTICLE INFO

Article history:
Received 7 June 2010
Received in revised form
6 August 2010
Accepted 15 October 2010
Available online 20 October 2010

Keywords:
Tidal flat
Flow in channels
Drag coefficient

ABSTRACT

Channels affect drainage and bed stresses on tidal flats. Here, near-bottom currents observed on a sandy tidal flat are compared with those observed 35 m away inside a shallow ($\approx$ 0.3 m deep) channel. For water depths between 0.5 and 2.5 m (when both current meters are submerged), current speeds 0.13 m above the bed on the flat are about 30% greater than those observed 0.13 m above the bed in the channel, and are approximately equal to those observed 0.58 m above the channel bed (0.26 m above the flat elevation). Flow directions on the flat are similar to those in the channel. For flows directed across the channel axis, the ratio of speeds increases from about 1.3 to about 2.2 with increasing water depth. The corresponding ratio of the vertical velocity variances (a proxy for turbulence) decreases from about 1.5 to about 0.2, suggesting that the turbulence near the bed of the channel is greater than that near the bed of the flat for water depths greater than about 1.0 m. Drag coefficients estimated with the vertical velocity variance are approximately 70% larger in the channel than over the visually smoother flat, consistent with prior studies suggesting that channels may increase tidal-flat roughness. For flows directed along the channel axis (in the cross-flat direction), the ratio of speeds (1.2) is similar to the ratio predicted by a cross-flat momentum (along-channel) balance.

1. Introduction

Tidal flats (Fig. 1) are found on coasts where there is a large supply of fine sediment, a large tidal range in water elevation, and low-to-moderate wave energy. Tidal flats also occur in areas with relatively small tidal ranges and sediment supply, such as Venice Lagoon (Day et al., 2004) and Hog Island Bay (Fugate et al., 2005). Healthy tidal flats are critical for many species of wading birds and coastal fish. Furthermore, tidal flats help protect coastal areas, both by providing a buffer at the shoreline and by influencing the coastal sediment budget. Tidal flats often are covered with dendritic branching channels (complex braids in Fig. 1) that direct both river water and ebbing tidal flows offshore and that may affect the hydraulic roughness of the flats (Whitehouse et al., 2000). Observations have suggested that the drainage density of tidal networks is related to channel width, cross-sectional area, discharge, and watershed area (Fagherazzi et al., 1999; Rinaldo et al., 1999). Numerical model simulations and a linear stability analysis of channels on short, wide mesotidal flats, such as those along the Dutch coast, suggest that the width and spacing of branching channels increase with increasing bottom slope, increasing Shield's number, and decreasing depth (Marciano et al., 2005).

Previous observations of tidal channels have focused on flows in marshes (Bayliss-Smith et al., 1979; Healy et al., 1981; Leopold et al., 1993; Fagherazzi et al., 2008), geomorphology (Bridges and Leeder, 1976; Fagherazzi and Furbish, 2001; Fagherazzi and Sun, 2004), internal waves (Adams et al., 1990), tidal constituents (Blanton et al., 2002), stratification (Ralston and Stacey, 2005a, b, 2006), and turbulence (Ralston and Stacey, 2005a, b, 2006). Numerical models suggest that flows in large channels are stronger than the flows across the flats (Fagherazzi et al., 2003; D'Alpaos et al., 2006), resulting in complicated patterns of circulation and channel-flat exchanges. Observations in a 0.5–1.2 m deep, 10 m wide channel and on the adjacent muddy tidal flat (Mariotti and Fagherazzi, in press) suggest that lateral flow toward the channel increases channel discharge as the flat drains during ebb tide. Although flows in the channel usually were low, pulses of strong along-channel flow were observed as the water level approached the elevation of the flat. Pulses during ebb tides were stronger than those during flood tides. Similar flows have been observed in salt marshes (Fagherazzi and Overeem, 2007, and references thererin).

Despite their potential importance as pathways for sediment transport (Wells et al., 1990; Christiansen et al., 2000; Hood, 2006; Green and Coco, 2007; Ralston and Stacey, 2007) and as roughness elements affecting the large-scale flow (Whitehouse et al., 2000), there are few observations of currents in small dendritic channels. In a small channel in the salt marshes and mudflats of San Francisco Bay, observations of currents were made along 3 cross-channel transects for two few-day (Ralston and Stacey, 2005b) and two 2-week periods (Ralston and Stacey, 2006). Owing to the curvature of the channel, the larger-scale flow changed from mostly along-channel to across-channel between the 3 transects, allowing

* Corresponding author. Tel.: +1 208 610 4333; fax: +1 240 248 4449.
E-mail addresses: elgar@whoi.edu (S. Elgar), britt@whoi.edu (B. Raubenheimer).

0278-4343/$ - see front matter © 2010 Elsevier Ltd. All rights reserved.
doi:10.1016/j.csr.2010.10.007

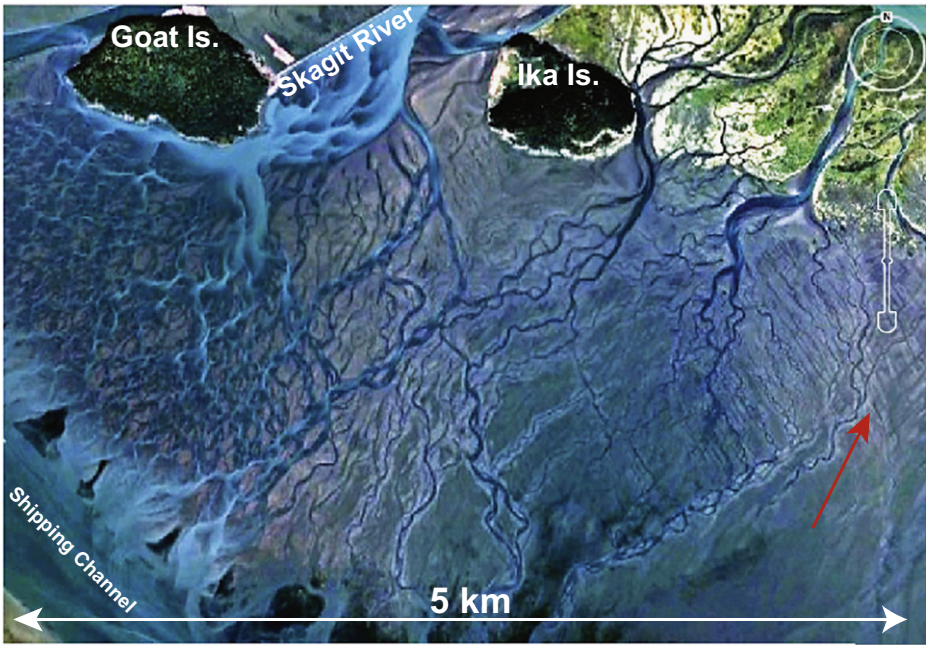

Fig. 1. Google Earth image of the north-western half of the Skagit Bay tidal flats, Puget Sound, WA at low tide. The discharge from the north fork of the Skagit River and the ebbing tidal flows are directed offshore toward the shipping channel by the 1/1000 slope of the tidal flat and by the numerous branching channels. The red arrow points to the location of sensors in a small channel and on the neighboring tidal flat discussed in the text.

investigation of flows with different orientations to the channel axis. Turbulence increased for across-channel flows, and for some conditions flows in the channel were smaller than those on the neighboring flat (Ralston and Stacey, 2005b, 2006).

Here, near-bed velocity observations obtained over a 6-week period on the sandy Skagit Bay tidal flat (Fig. 1) are compared with flows observed in a nearby small channel. Tidal flow directions rotated 360° counterclockwise during each tidal cycle, enabling the effect of flow direction on current speed and turbulence to be examined at a single location.

2. Field observations

Observations of velocity and pressure were obtained in a small channel and on the neighboring tidal flat (Figs. 2 and 3) in Skagit Bay, Puget Sound, WA (Fig. 1) between July 20 and August 28, 2009. The channel axis was aligned approximately across the flat (Fig. 2). Two near-bed acoustic Doppler velocimeters and an acoustic Doppler profiler (Fig. 3) were sampled continuously at 2 Hz, and the data were subdivided into 512 s (8.5 min) subsections for which mean velocities and pressures were calculated. The tidal range in Skagit Bay is approximately 4 m, and at the mid-flat location of the instruments the range is about 2.5 m. The current meters required approximately 0.25 m water depth to operate. After discarding data when the current meter on the flats was not submerged owing to low tides, and when sensors were fouled by algal mats (despite daily cleaning) or were being maintained, approximately 1800 subsections of data were available for analysis.

Cross-channel (along-flat) velocities reach a local maximum near the middle of the flood tide, reverse their direction and reach a maximum in the opposite direction near high tide, then slowly decrease as the tide ebbs (Fig. 4B). In contrast, similar to flows in a swash zone on a beach (Raubenheimer, 2002), along-channel (across-flat) velocities are maximum near the beginning of the flood, decrease to zero at high tide, then steadily increase in the opposite direction as the tide ebbs, reaching another maximum

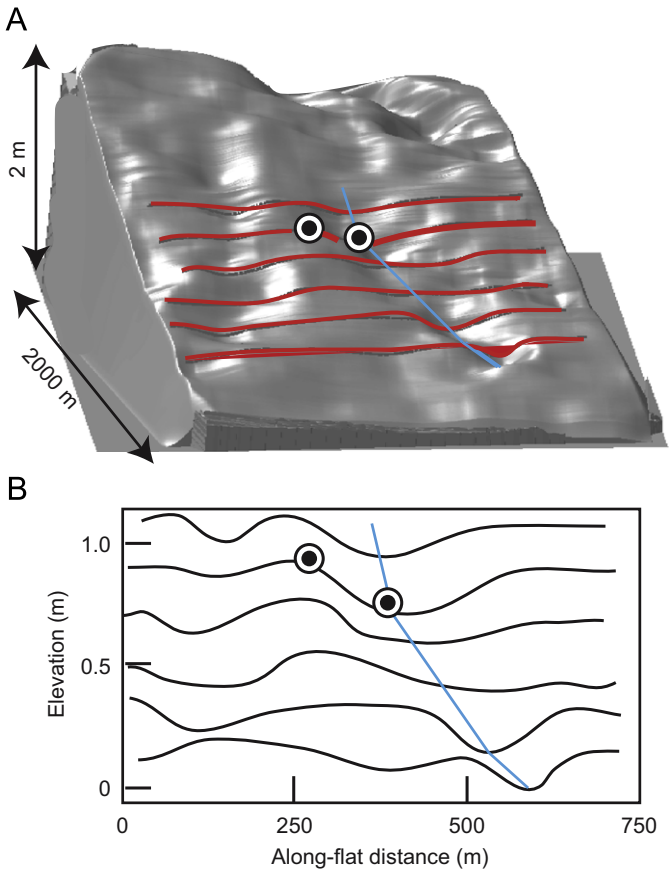

Fig. 2. (A) 750 m along-flat by 2000 m cross-flat section of the tidal flat surrounding the small channel (blue curve) discussed in the text. There is approximately 2 m change in elevation across this section of the tidal flat. (B) Elevation versus along-flat distance for the 6 transects indicated by the red curves in A. The symbols are approximate instrument locations. The bathymetric data were obtained with a sonar and GPS mounted on a jet ski.

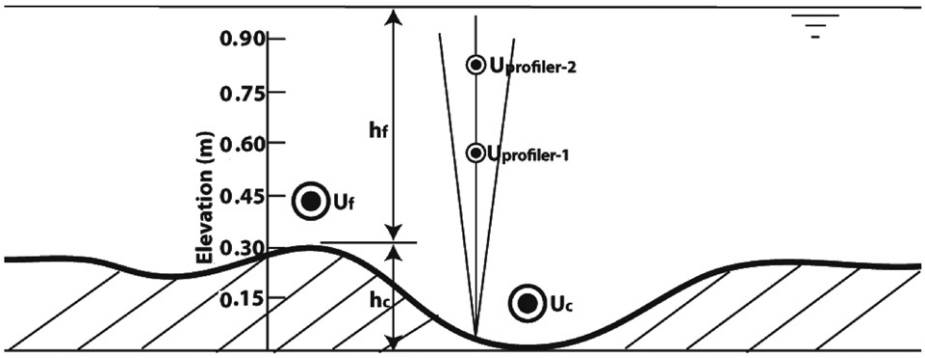

Fig. 3. Instrument locations on the tidal flat and in the channel. Large circles are sample volumes of acoustic Doppler current meters, and small circles are sample volumes in the lowest two bins of an acoustic Doppler current profiler. Pressure gages were colocated with each current meter. The total water depth in the channel is h_f+h_c, where h_f is the depth of water above the flat and h_c is the depth of the channel below the flat.

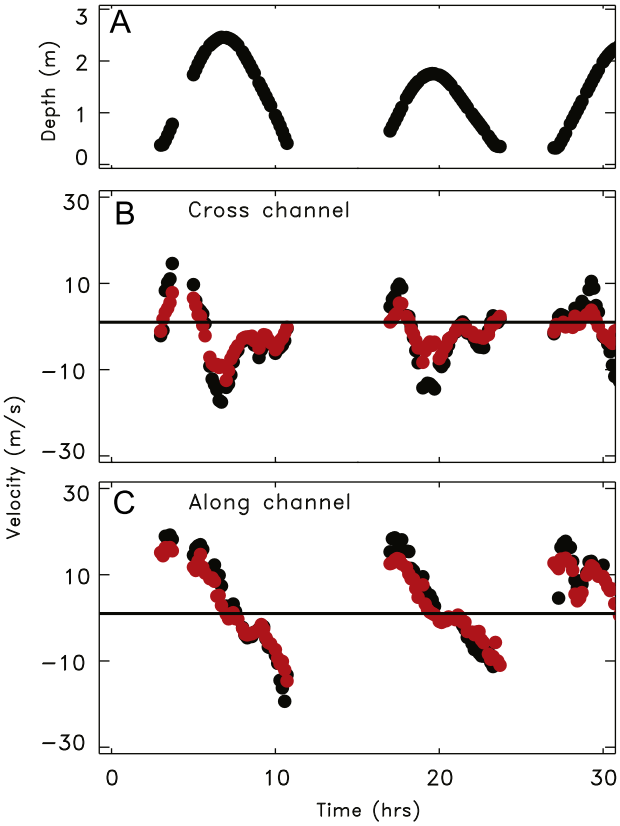

Fig. 4. (A) Water depth, (B) cross-channel velocity, and (C) along-channel velocity versus time. Black symbols in B and C are velocities observed 0.13 m above the bed on the tidal flat, and red symbols are velocities observed 0.13 m above the bed of the channel. There are no data at low tide when the sensors were not submerged (e.g., 11 < time < 16 h) and when the sensors were fouled with seaweed (e.g., near time = 4 h).

near low tide (Fig. 4C). As described below for the full data set, the velocities observed above the tidal flat are stronger than those observed above the channel bed (Fig. 4).

Hourly boundary finding by the downward-looking acoustic current meters, almost-daily low-tide visual observations, CTD casts, and occasional large-scale bathymetric surveys indicate the channel bed ranged from approximately 0.20 to 0.35 m below the surface of the tidal flat between June 28 and July 20 (when the flow measurements begin), at which time the channel depth stabilized (until August 28) to about 0.30–0.35 m below the flat level. River discharge decreased from about 475 m^3/s on June 28 to about 345 m^3/s on July 20 and about 170 m^3/s on August 28, of which approximately 60% flows through the north fork of the Skagit River, primarily via the main channel between Goat and Ika islands (Fig. 1). (The south fork of the Skagit River (not shown) discharges onto the flats about 15 km south of the study region). River discharge is a small fraction of the tidal prism during the period investigated here.

3. Results

Flow directions observed on the flat were similar to those observed in the channel (Fig. 5A). However, across-channel flows observed on the flat were about 40% greater than those observed in the channel (Fig. 5B), and along-channel flows on the flat were about 20% greater than those observed in the channel (Fig. 5C). Unlike observations in a deeper (1–1.5 m deep, 1 m wide) channel on a muddy tidal flat (Mariotti and Fagherazzi, in press) and in much larger (> 1 m deep, 100 m wide) channels on both muddy and sandy tidal flats (Ogston et al., 2010; Geyer et al., 2010), strong pulses of flow in the channel during ebb tide were not observed, neither when both sensors were submerged (Fig. 5) nor when water levels dropped below the elevation of the flat (not shown). The lack of a strong ebb tide pulse may be owing to the relatively small river discharge in the channel studied here, which was not bank-full at low tide. Moreover the slope of the channel studied here was less than the slope of the tidal flat, and thus unlike the deeper channels (Mariotti and Fagherazzi, in press; Ogston et al., 2010; Geyer et al., 2010), the channel disappeared into the tidal flat about 1000 m offshore of the instrument locations (Fig. 2). Low-tide visual observations of wide areas of shallow (0.1 m deep) water flowing seaward near the outer edge of the flat approximately 2000 m offshore of the instruments are consistent with decreased channelization of water.

The ratio of current speed (defined as the square root of the sum of the squared along- and across-channel flows) observed 0.13 m above the bed on the flat, U_f, to that observed 0.13 m above the bed in the channel, U_c, increases as the direction of flow rotates from along ($\theta = 0°$, where θ is the angle between flow direction and along-channel orientation) to across ($\theta = 90°$) channel (filled circles in Fig. 6). However, flows observed about 0.58 m above the channel bed (0.26 m above the flat elevation) (profiler-1 in Fig. 3) are approximately the same as those observed 0.13 m above the flat (open squares in Fig. 6). Flows 0.83 m above the channel bed (0.51 m above the flat elevation) (profiler-2 in Fig. 3) are stronger than those observed 0.13 m above the flat (filled triangles, Fig. 6), consistent with increasing flow speeds with increasing distance above the bottom boundary layer. The ratio U_f/U_c is insensitive to

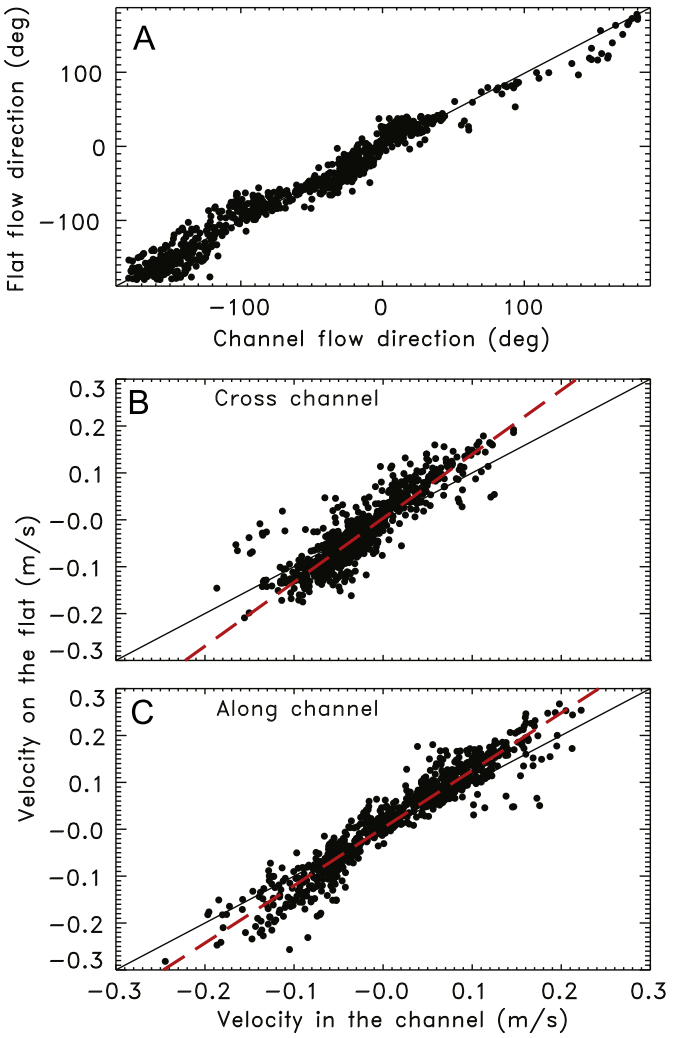

Fig. 5. (A) Direction of flow observed 0.13 m above the tidal flat versus direction of flow observed 0.13 m above the channel bed, and velocity observed on the flat versus velocity observed in the channel for flows (B) across and (C) along the channel axis. The solid lines are 1-to-1 correspondences, and red dashed lines are least squares fits through the data with slopes of 1.4 (B) and 1.2 (C).

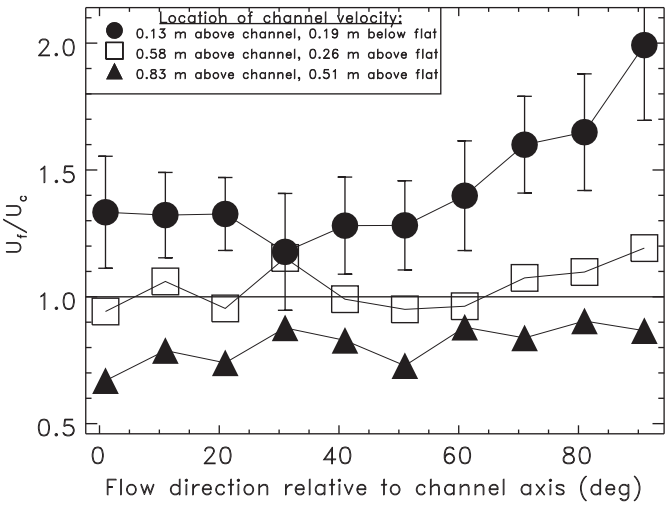

Fig. 6. Ratio of current speed observed on the tidal flat to that observed in the channel versus flow direction relative to the channel axis. Observations were obtained approximately 0.13 m above the bed of the tidal flat, and 0.13 (filled circles), 0.58 (open squares), and 0.83 m (filled triangles) above the bed of the channel. Bars are 1 standard deviation of the acoustic Doppler velocimeter data. Standard deviations for the acoustic Doppler profilers are similar, but somewhat larger.

the flow direction when U_c is measured 0.58 m or more above the channel bed (Fig. 6).

The magnitudes of maximum across- and along-channel flows are similar for both rising and falling tides (Fig. 4), as is the ratio U_f/U_c. The ratio also is similar for spring and neap tides, although flows are somewhat stronger during springs than during neaps.

For currents flowing primarily across the channel ($60^\circ < \theta < 90^\circ$), U_f/U_c increases as the depth increases (Fig. 7A). Assuming that vertical velocity fluctuations are a proxy for turbulence, it can be shown that (Nezu and Rodi, 1986):

$$\langle w'w' \rangle \approx C_d U^2 \quad (1)$$

where w' is the turbulent fluctuation of the vertical velocity, angled brackets mean time average, C_d is the drag coefficient, and U is the flow speed. Here, wave motions are negligible, and $\langle w'w' \rangle$ is approximated as the variance of the vertical velocity, var(w). Least squares fits to var(w) versus U^2 for all flow directions (not shown, correlation coefficients, r^2 were between 0.7 and 0.9) result in estimates of the drag coefficient of $C_d = 0.003$ on the tidal flat and $C_d = 0.005$ in the channel. The high correlation coefficients and the similarity of the estimated drag coefficients to previous results, which range from about 0.002 to 0.008 (Collins et al., 1998; Verney et al., 2006, and many others), suggests that var(w) can be used as a proxy for turbulence levels for the data discussed here.

The increase of U_f/U_c with depth is accompanied by an increase in the relative amount of turbulence near the channel bed (Fig. 7B), consistent with previous observations of flows across a channel (Ralston and Stacey, 2005b, 2006). Unlike previous studies (Ralston and Stacey, 2005b, 2006), vertical profiles of conductivity and temperature (i.e., the vertical structure of density) measured over the channel were similar to those measured over the neighboring flat. The decreased across-channel flows in the channel relative to those on the neighboring flats may be caused by increased generation of turbulence at the edges of the channel (Ralston and Stacey, 2005b), a separation zone near the channel bottom, or increased drag over the rougher channel bed. Visual observations suggest the tidal flat bed was smooth, whereas the channel had numerous randomly aligned bedforms and algal mats with heights of up to about 0.25 m. Thus, the higher turbulence levels and larger drag coefficients in the channel relative to the flats may be related to the channel roughness (Whitehouse et al., 2000). These conditions, which are opposite to the smooth channels and rougher flat surfaces observed on muddy tidal flats (Mariotti and Fagherazzi, in press), are consistent with the hypothesis that channels cause increased hydraulic roughness on sandy tidal flats (Whitehouse et al., 2000).

In contrast to across-channel flows, when the flow is primarily along the channel ($0^\circ < \theta < 40^\circ$), the ratio U_f/U_c is only weakly dependent on water depth (Fig. 7C), as is the ratio var(w_f)/var(w_c) (Fig. 7D).

The ratio U_f/U_c observed for along-channel flows (Figs. 5C and 6) is consistent with a cross-shore momentum balance. For unidirectional across-flat (i.e., along-channel) flows without secondary circulation or along-flat (across-channel) gradients, prior studies (Le Hir et al., 2000; Ertürk et al., 2002; Zippel et al., 2010) have suggested that the cross-flat momentum balance is dominated by the barotropic pressure gradient and bottom stress such that

$$gh\partial\eta/\partial x = C_d U^2 \quad (2)$$

where g is the gravitational acceleration, h the water depth, η the sea surface elevation relative to the mean sea surface level, x the cross-flat distance, and U the cross-flat flow speed. For these

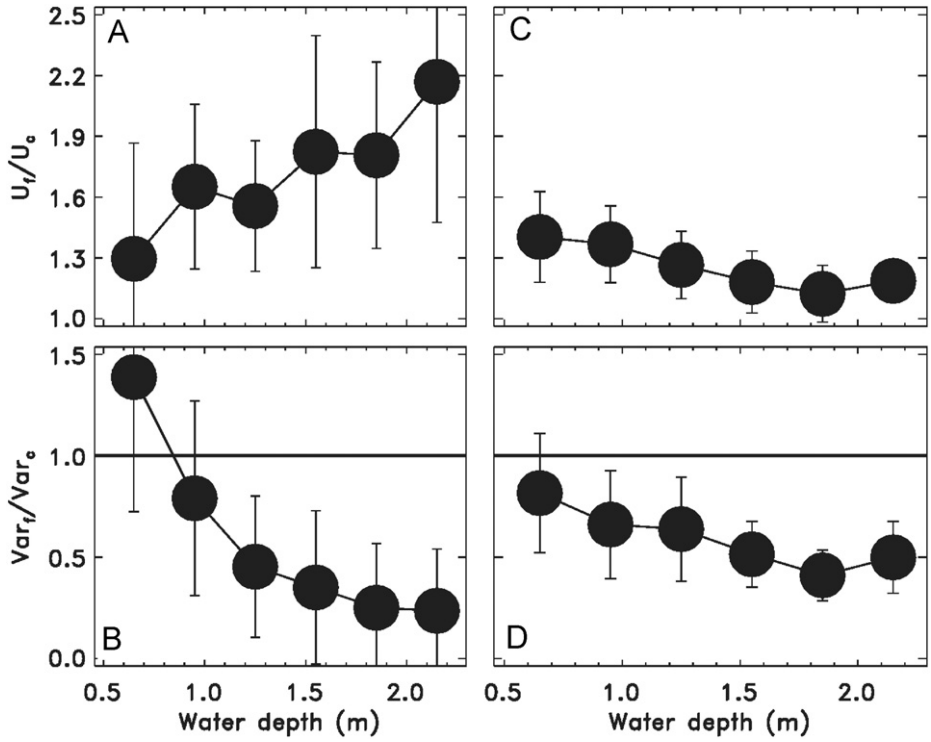

Fig. 7. Ratio of current speed and vertical velocity variance observed on the flat to that observed in the channel versus water depth on the flat for (A–B) flow directions greater than 60° relative to the channel axis (across-channel flow) and (C–D) flow directions within 40° of the channel axis (along-channel flow). Bars are 1 standard deviation.

assumptions, $\partial\eta/\partial x$ is the same over the flat and the channel. For an average water depth on the flat of 1.2 m, a 0.3 m deep channel, and drag coefficients of 0.003 on the flat and 0.005 in the channel, Eq. (2) implies $U_f/U_c \approx 1.2$, similar to the observed ratio of 1.2 (Figs. 5C and 6).

4. Conclusions

Mean currents observed near the bed on a sandy tidal flat were larger than the currents observed near the bed in a nearby small dendritic channel. For flows directed across the channel axis, currents were 40% larger on the flat than in the channel. As the water depth increased, cross-channel flows on the flat increased relative to those in the channel, and vertical velocity fluctuations on the flat decreased relative to those in the channel. Bottom drag coefficients estimated using vertical velocity fluctuations as a proxy for turbulence are about 70% larger in the channel than on the flat. For flows directed along the channel axis, currents were 20% larger on the flat than in the channel, and the ratio of these flow speeds is consistent with a cross-flat (along-channel) momentum balance.

Acknowledgements

We thank W. Boyd, D. Darnell, D. Giffen, L. Gorrell, S. Kilgallin, E. Ladouceur, V. Pavel, E. Williams, R. Yopak, and S. Zippel for helping obtain the field observations, J. Trowbridge, D. Ralston, R. Geyer, and S. Lentz for many useful suggestions and discussions, G. Mariotti and S. Fagherazzi for sharing their preliminary results and insight, and both anonymous referees for many excellent recommendations and questions. The Office of Naval Research, the National Science Foundation, and a National Security Science and Engineering Faculty Fellowship provided support.

References

Adams Jr., C., Wells, J., Park, Y., 1990. Internal hydraulics of a sediment-stratified channel flow. Marine Geology 95, 131–145.
Bayliss-Smith, T., Healey, R., Lailey, R., Spencer, T., Stoddart, R., 1979. Tidal flows in salt marsh creeks. Estuarine and Coastal Marine Science 9, 235–255.
Blanton, J., Lin, G., Elston, S., 2002. Tidal current asymmetry in shallow estuaries and tidal creeks. Continental Shelf Research 22, 1731–1743.
Bridges, P., Leeder, M., 1976. Sedimentary model for intertidal mudflat channels, with examples from Solway Firth, Scotland. Sedimentology 23 (4), 533–552.
Christiansen, T., Wiberg, P., Mulligan, T., 2000. Flow and sediment transport on a tidal salt marsh surface. Estuarine, Coastal, and Shelf Science 50, 315–331.
Collins, M., Ke, X., Gao, S., 1998. Tidally-induced flow structure over intertidal flats. Estuarine, Coastal, and Shelf Science 46, 233–250.
D'Alpaos, A., Lanzoni, S., Mudd, S., Fagherazzi, S., 2006. Modeling the influence of hydroperiod and vegetation on the cross-sectional formation of tidal channels. Estuarine, Coastal, and Shelf Science 69 (3–4), 311–324.
Day, J., Rismondo, A., Scarton, F., Are, D., Cecconi, G., 2004. Relative sea-level rise and Venice lagoon wetlands. Journal of Coastal Conservation 4, 27–34.
Ertürk, S., Bilgili, A., Swift, M., Brown, W., Çelikkol, B., Ip, J., Lynch, D., 2002. Simulation of the Great Bay estuarine system: tides with tidal flat wetting and drying. Journal of Geophysical Research, 107. doi:10.1029/2001JC000883.
Fagherazzi, S., Bortoluzzi, A., Dietrich, W., Adami, A., Lanzoni, S., Marani, M., Rinaldo, A., 1999. Tidal networks: 1. Automatic network extraction and preliminary scaling features from digital terrain maps. Water Resources Research 35, 3891–3904.
Fagherazzi, S., Furbish, D., 2001. On the shape and widening of salt marsh creeks. Journal of Geophysical Research 106, 991–1003.
Fagherazzi, S., Wiberg, P., Howard, A., 2003. Tidal flow field in a small basin. Journal of Geophysical Research, 108. doi:10.1029/2002JC001340.
Fagherazzi, S., Sun, T., 2004. A stochastic model for the formation of channel networks in tidal marshes. Geophysical Research Letters 31 (21. doi:10.1029/2004GL020965.
Fagherazzi, S., Overeem, I., 2007. Models of deltaic and inner continental shelf landform evolution. Annual Review of Earth and Planetary Sciences 35, 685–715.
Fagherazzi, S., Hannion, M., D'Odorico, P., 2008. Geomorphic structure of tidal hydrodynamics in salt marsh creeks. Water Resources Research 44 (2. doi:10.1029/2007WR006289.
Fugate, D., Friedrichs, C., Bilgili, A., 2005. Estimation of residence time in a shallow back barrier lagoon, Hog Island Bay, Virginia, USA. ASCE Conference Proceedings 209, 19. doi:10.1061/40876(209)19.
Geyer, R., Ralston, D., Traykovski, P., 2010. The dynamics of channels on Skagit tidal flats. EOS Transactions AGU 91 (26) Ocean Science Meeting Supplement, Abstract GO34A-01.

Green, M., Coco, G., 2007. Sediment transport on an estuarine intertidal flat: measurements and conceptual model of waves, rainfall and exchanges with a tidal creek. Estuarine, Coastal, and Shelf Science 72, 553–569.

Healy, R., Pye, K., Stoddart, D., Bayliss-Smith, T., 1981. Velocity variations in salt marsh creeks, Norfolk, England. Estuarine, Coastal, and Shelf Science 13, 535–545.

Hood, W., 2006. A conceptual model of depositional, rather than erosional, tidal channel development in the rapidly prograding Skagit River Delta (Washington, USA). Earth Surface Processes and Landforms 31 (14), 1824–1838.

Le Hir, P., Roberts, W., Cazaillet, O., Christie, M., Bassoullet, P., Bacher, C., 2000. Characterization of intertidal flat hydrodynamics. Continental Shelf Research 20, 1433–1459.

Leopold, L., Collins, J., Collins, L., 1993. Hydrology of some tidal channels in estuarine marshland near San Francisco. Catena 20 (5), 469–493.

Marciano, R., Wang, Z., Hibma, A., de Vriend, H., 2005. Modeling of channel patterns in short tidal basins. Journal of Geophysical Research 110. doi:10.1029/2003JF000092.

Mariotti, G., Fagherazzi, S., Hydrodynamics of a tidal channel in a mesotidal mudflat, Continental Shelf Research, in press. doi:10.1016/j.csr.2010.10.014.

Nezu, I., Rodi, W., 1986. Open-channel flow measurements with a laser Doppler anemometer. Journal of Hydraulic Engineering 112 (5), 335–355.

Ogston, A., Nowacki, D., Lee, K., Boldt, K., 2010. Role of channel morphology on channel-flat sediment-transport dynamics of tidal flats. EOS Transactions AGU 91 (26) Ocean Science Meeting Supplement, Abstract GO34A-03.

Ralston, D., Stacey, M., 2005a. Longitudinal mixing and lateral circulation in the intertidal zone. Journal of Geophysical Research 110, C07015. doi:10.1029/2005JC002888.

Ralston, D., Stacey, M., 2005b. Stratification and turbulence in subtidal channels through intertidal mudflats. Journal of Geophysical Research 110, C08009. doi:10.1029/2004JC002650.

Ralston, D., Stacey, M., 2006. Shear and turbulence production across subtidal channels. Journal of Marine Research 64, 147–171.

Ralston, D., Stacey, M., 2007. Tidal and meteorological forcing of sediment transport in tributary mudflat channels. Continental Shelf Research 27, 1510–1527.

Raubenheimer, B., 2002. Observations and predictions of fluid velocities in the surf and swash zones. Journal of Geophysical Research 107, 3190. doi:10.1029/2001JC001264.

Rinaldo, A., Fagherazzi, S., Lanzoni, S., Marani, M., Dietrich, W., 1999. Tidal networks 3. Landscape-forming discharges and studies in empirical geomorphic relationships. Water Resources Research 35 (12), 3919–3929.

Verney, R., Brun-Cottan, J., Lafite, R., Deloffre, J., Taylor, J., 2006. Tidally induced shear stress variability above intertidal mudflats in the macrotidal Seine Estuary. Estuaries and Coasts 29 (4), 653–664.

Wells, J., Adams, C., Park, T., Frankenberg, E., 1990. Morphology, sedimentology, and tidal channel processes on a high-tide-range mudflat, west coast of South Korea. Marine Geology 95, 111–130.

Whitehouse, R., Bassoullet, P., Dyer, K., Mitchener, H., Roberts, W., 2000. The influence of bedforms on flow and sediment transport over intertidal mudflats. Continental Shelf Research 20 (10–11), 1099–1124.

Zippel, S., Raubenheimer, B., Elgar, S., 2010. Bottom drag coefficients on a tidal flat. EOS Transactions AGU 91 (26) Ocean Science Meeting Supplement, Abstract GO35C-06.